Geophys. J. Int. (2008) **174,** 316–330 doi: 10.1111/j.1365-246X.2008.03812.x

Ray tracing and inhomogeneous dynamic ray tracing for anisotropy specified in curvilinear coordinates

Einar Iversen[1] and Ivan Pšenčík[2]

[1]*NORSAR,* PO Box 53, 2027 *Kjeller, Norway. E-mail:einar.iversen@norsar.com*
[2]*Institute of Geophysics, Acad. Sci. of Czech Republic, Boční II,* 141 31 *Praha* 4, *Czech Republic. E-mail: ip@ig.cas.cz*

Accepted 2008 April 4. Received 2008 March 25; in original form 2007 September 3

SUMMARY

Ray tracing has recently been expressed for anisotropy specified in a local Cartesian coordinate system, which may vary continuously in a model specified by elastic parameters. It takes advantage of the fact that anisotropy is often of a simpler nature locally (and is thus specified by a smaller number of elastic parameters) and that the orientation of its symmetry elements may vary. Here we extend this approach by replacing the local Cartesian coordinate system with a curvilinear coordinate system of global extent and by applying the new approach to ray tracing and inhomogeneous dynamic ray tracing. The curvilinear coordinate system is orthogonal and is constructed so that the coordinate axes are consistent with the considered anisotropy of the medium. Our formulation allows for computation of ray attributes (e.g. ray velocity vector and paraxial ray attributes) in the curvilinear coordinate system, while rays are computed in global Cartesian coordinates. Compared to the classic formulation in terms of 21 elastic moduli in global Cartesian coordinates, the main advantages are improved efficiency, lower computer-memory requirements, and conservation of anisotropic symmetry throughout the model.

Key words: Body waves; Seismic anisotropy; Wave propagation.

1 INTRODUCTION

In recent years, modelling and imaging in the presence of highly complicated anisotropic structures of general orientation has drawn increased interest (e.g. Vestrum *et al.* 1999; Isaac & Lawton 1999; Lanlan *et al.* 2004; Dehghan *et al.* 2007). The objective of this paper is to formulate ray tracing and dynamic ray tracing procedures, applicable to such complicated structures, and thereby to take advantage of local anisotropy properties, so that modelling can be performed faster and using less memory as compared to conventional approaches for ray tracing and dynamic ray tracing.

Iversen & Pšenčík (2007) proposed a ray tracing procedure, in which anisotropy was specified in a local Cartesian coordinate system varying continuously in a model specified by elastic parameters (referred to as the 'model' in the following). In this paper, we replace the local Cartesian coordinate system by an orthogonal curvilinear coordinate system of global extent and generalize the procedure to include inhomogeneous dynamic ray tracing (Červený 2001, section 4.3.8), which plays an important role in the ray perturbation methods. The main motive for introducing the curvilinear coordinate system is the same as in Iversen & Pšenčík (2007): to reduce the number of volumetric model functions required to simulate wave propagation in a realistic model with higher-symmetry anisotropy. The basic symmetry elements, for example, the symmetry axis of a transversely isotropic (TI) medium or symmetry planes of an orthorhombic (OR) medium, are allowed to vary spatially. A major reduction of the number of involved volumetric model function evaluations has a significant impact on the efficiency of computations as well as on the computer memory requirements. Furthermore, if we ensure, for example, that the symmetry axis of a TI medium is always parallel to a selected coordinate axis of the curvilinear coordinate system, or that any symmetry plane of an OR medium is always normal to a coordinate axis of the curvilinear coordinate system, conservation of anisotropic symmetry is implicitly guaranteed. In this way, the above-proposed scheme leads to easier physical interpretability of the model and to significant reduction of the number of parameters to be solved for in possible inversions. The effect of using a global curvilinear coordinate system in the context of continuously varying anisotropy is equivalent to using a local Cartesian coordinate system with continuously changing orientations of the axes; see Iversen & Pšenčík (2007). However, by introducing curvilinear coordinates the derivation of inhomogeneous dynamic ray tracing turned out to be easier.

The reformulated ray tracing and dynamic ray tracing equations presented here are valid for any kind of anisotropy. Their broadest application, however, is expected in media of higher anisotropic symmetry such as TI or OR symmetry. The reformulated ray tracing and

dynamic ray tracing have several advantages: faster computations, lower memory requirements, enhanced user-friendliness, and conservation of anisotropic symmetry properties in evaluating the material parameters at an arbitrary point of the model. The latter is not guaranteed for standard ray tracing and dynamic ray tracing based on the evaluation of 21 elastic moduli given in Cartesian coordinates. A basic assumption in our approach is that elastic moduli belonging to the curvilinear coordinate system are C2 continuous functions of the Cartesian coordinates. In addition, we assume to have access to a number of functions parametrizing the transformation between curvilinear and Cartesian coordinates everywhere within the region of interest. As with the elastic moduli, such functions must be C2 continuous in the Cartesian coordinate system.

The paper is organized as follows. We first introduce coordinate systems and specify relations between them. Then, we review ray tracing and inhomogeneous dynamic ray tracing in Cartesian coordinates. A mixed phase-space domain, formed by the Cartesian position vector and the slowness vector in curvilinear coordinates plays a basic role. One section is devoted to the slowness vector in curvilinear coordinates and its derivatives. The next task is to express the right-hand sides of the ray tracing and inhomogeneous dynamic ray tracing equations in terms of coefficients evaluated in the mixed phase-space domain. This leads to a set of transformation relations representing the final result of the paper. The accuracy of the proposed procedure is illustrated for models with TI and OR symmetry.

We use mostly component notation. The Einstein summation convention is used for repeated subscripts. Indices $i, j, \ldots, m, n$ run from 1 to 3; indices α and β run from 1 to 6.

2 COORDINATE SYSTEMS

In Sections 2.1 and 2.2, we describe two coordinate systems of importance to the context of this paper and also introduce phase spaces associated with these coordinate systems. Sections 2.3 and 2.4 are devoted to the transformation between the two coordinate systems. Finally, in Section 2.5, we introduce ray coordinates.

2.1 Cartesian coordinate system

Consider a Cartesian coordinate system, $\mathbf{x} \equiv (x_1, x_2, x_3)$. The elastic moduli belonging to this coordinate system are denoted equivalently in standard tensor notation, $a^{(x)}_{ijkl}$, or in the Voigt notation, $A^{(x)}_{\alpha\beta}$. Let τ denote the traveltime for a selected elementary wave, and let slowness vector $\mathbf{p}^{(x)}$ in the Cartesian coordinate system be defined by

$$p_i^{(x)} = \frac{\partial \tau}{\partial x_i}. \tag{1}$$

The phase space associated with the Cartesian coordinate system is 6-D with coordinates x_i and $p_i^{(x)}$.

2.2 Curvilinear coordinate system

Consider a curvilinear coordinate system, $\boldsymbol{\xi} \equiv (\xi_1, \xi_2, \xi_3)$, with curved orthogonal axes. The origin, $(\xi_1, \xi_2, \xi_3) = (0, 0, 0)$ is fixed relative to the Cartesian coordinate system, (x_1, x_2, x_3). Elastic moduli belonging to the curvilinear coordinate system are denoted $a^{(\xi)}_{ijkl}$ in standard tensor notation and $A^{(\xi)}_{\alpha\beta}$ in the Voigt notation. Slowness vector $\mathbf{p}^{(\xi)}$ in curvilinear coordinates is defined as

$$p_i^{(\xi)} = \frac{\partial \tau}{\partial \xi_i}, \tag{2}$$

where τ again stands for the traveltime as in eq. (1). As with Cartesian coordinates, the phase space formed by ξ_i and $p_i^{(\xi)}$ is 6-D.

The specification of the curvilinear coordinate system depends on the type of anisotropy. For a TI medium it is natural to let one of the coordinate axes be parallel to the axis of symmetry everywhere. As a consequence, the remaining two axes will be mutually perpendicular in the plane perpendicular to the symmetry axis. Similarly, for an OR medium one will typically require the coordinate lines to be perpendicular to symmetry planes at any point.

2.3 Transformation matrix H

Matrices for the transformation from curvilinear coordinates (ξ_1, ξ_2, ξ_3) to Cartesian coordinates (x_1, x_2, x_3) and vice versa, are denoted $\mathbf{H}$ and $\bar{\mathbf{H}}$, respectively, where $\bar{\mathbf{H}} = \mathbf{H}^{-1}$. The matrix elements,

$$H_{ij}(\boldsymbol{\xi}) = \frac{\partial x_i}{\partial \xi_j}, \qquad \bar{H}_{jk}(\mathbf{x}) = \frac{\partial \xi_j}{\partial x_k}, \tag{3}$$

satisfy the relation

$$H_{ij}\bar{H}_{jk} = \delta_{ik}. \tag{4}$$

Since the curvilinear coordinate system is orthogonal, we have

$$\bar{\mathbf{H}} = \mathbf{H}^{-1} = \mathbf{H}^T, \tag{5}$$

and thus

$$\bar{H}_{jk} = H_{kj}. \tag{6}$$

Hereinafter, a one-to-one relationship is assumed between coordinates $\mathbf{x}$ and $\boldsymbol{\xi}$, that is, we require single-valued functions $\mathbf{x}(\boldsymbol{\xi})$ and $\boldsymbol{\xi}(\mathbf{x})$ to exist in the $\boldsymbol{\xi}$ and $\mathbf{x}$ domains. This means that we can express matrix $\mathbf{H}$ as a single-valued function of $\mathbf{x}$:

$$\mathbf{H} = \mathbf{H}(\mathbf{x}). \tag{7}$$

2.4 Parametrization of matrix H

Transformation matrix $\mathbf{H}$ is assumed to be accessible everywhere in the region of interest as a continuous function with continuous first- and second-order derivatives. Matrix $\mathbf{H}$ can be parametrized by three parameters. As in Iversen & Pšenčík (2007), we use three Euler angles λ, μ and ν as the parametrizing functions. This yields the relation

$$\mathbf{H} = \begin{pmatrix} \cos\lambda\cos\nu + \sin\lambda\sin\mu\sin\nu & -\cos\lambda\sin\nu + \sin\lambda\sin\mu\cos\nu & \sin\lambda\cos\mu \\ \cos\mu\sin\nu & \cos\mu\cos\nu & -\sin\mu \\ -\sin\lambda\cos\nu + \cos\lambda\sin\mu\sin\nu & \sin\lambda\sin\nu + \cos\lambda\sin\mu\cos\nu & \cos\lambda\cos\mu \end{pmatrix}. \tag{8}$$

The angles λ, μ and ν may vary from point to point. In models of TI symmetry, the angles λ and μ yield the orientation of the symmetry axis, and the angle ν can be chosen arbitrarily.

2.5 Ray coordinates

Rays can be specified by two quantities, γ_1 and γ_2, called '*ray parameters*'. Examples of such parameters are two components of the position vector along an initial surface, two components of the slowness vector or two take-off angles at a selected point on a ray. The ray parameters and a third quantity, γ_3, a monotonic parameter along the ray, represent '*ray coordinates*' γ_1, γ_2, γ_3. In the following, the traveltime τ is used exclusively as the parameter γ_3. Ray coordinates are of particular importance in dynamic ray tracing.

3 CHRISTOFFEL MATRIX AND HAMILTONIANIN CARTESIAN PHASE SPACE

In Cartesian phase-space coordinates, the elements of the Christoffel matrix are:

$$\Gamma_{ik}^{(x)}\left[\mathbf{x}, \mathbf{p}^{(x)}\right] = a_{ijkl}^{(x)}(\mathbf{x}) p_j^{(x)} p_l^{(x)}. \tag{9}$$

A selected eigenvalue, $G^{(x)}$, of the Christoffel matrix can be expressed, see, for example, Červený (2001), as

$$G^{(x)}\left[\mathbf{x}, \mathbf{p}^{(x)}\right] = \Gamma_{ik}^{(x)}\left[\mathbf{x}, \mathbf{p}^{(x)}\right] g_i^{(x)}\left[\mathbf{x}, \mathbf{p}^{(x)}\right] g_k^{(x)}\left[\mathbf{x}, \mathbf{p}^{(x)}\right], \tag{10}$$

where it is understood that the components of the corresponding eigenvector, $\mathbf{g}^{(x)}$, are $g_i^{(x)}$. We require that eigenvalue $G^{(x)}$ satisfies the eikonal equation:

$$G^{(x)} = 1. \tag{11}$$

Based on eigenvalue $G^{(x)}$, one can define the Hamiltonian function corresponding to traveltime τ as a variable along the ray:

$$\mathcal{H}^{(x)}\left[\mathbf{x}, \mathbf{p}^{(x)}\right] = \frac{1}{2}\left\{G^{(x)}\left[\mathbf{x}, \mathbf{p}^{(x)}\right] - 1\right\}. \tag{12}$$

The partial derivatives of Hamiltonian $\mathcal{H}^{(x)}$ and of eigenvalue $G^{(x)}$ are related by

$$\frac{\partial \mathcal{H}^{(x)}}{\partial x_i} = \frac{1}{2}\frac{\partial G^{(x)}}{\partial x_i}, \qquad \frac{\partial \mathcal{H}^{(x)}}{\partial p_i^{(x)}} = \frac{1}{2}\frac{\partial G^{(x)}}{\partial p_i^{(x)}}, \tag{13}$$

and so forth for higher-order derivatives.

4 RAY TRACING AND INHOMOGENEOUS DYNAMIC RAY TRACING IN CARTESIAN COORDINATES

4.1 Ray tracing equations

Ray tracing in Cartesian coordinates is governed by a system of differential equations for position vector $\mathbf{x}$ and slowness vector $\mathbf{p}^{(x)}$:

$$\frac{\mathrm{d}}{\mathrm{d}\tau}\begin{bmatrix} \mathbf{x} \\ \mathbf{p}^{(x)} \end{bmatrix} = \begin{bmatrix} \mathbf{v}^{(x)} \\ \boldsymbol{\eta}^{(x)} \end{bmatrix}. \tag{14}$$

In eq. (14), traveltime τ is the variable along the ray, and $\mathbf{v}^{(x)}$ and $\boldsymbol{\eta}^{(x)}$ are the so-called ray velocity vector and $\boldsymbol{\eta}$ vector, with components

$$v_i^{(x)} = \frac{1}{2}\frac{\partial G^{(x)}}{\partial p_i^{(x)}}, \qquad \eta_i^{(x)} = -\frac{1}{2}\frac{\partial G^{(x)}}{\partial x_i}. \tag{15}$$

4.2 Inhomogeneous dynamic ray tracing equations

The inhomogeneous dynamic ray tracing system in Cartesian coordinates (Červený 2001, eq. 4.3.40) is formulated by the following system of linear differential equations:

$$\frac{\mathrm{d}}{\mathrm{d}\tau}\begin{bmatrix}\mathbf{Q}\\ \mathbf{P}\end{bmatrix} = \begin{pmatrix}\boldsymbol{\mathcal{S}}^T & \boldsymbol{\mathcal{T}}\\ -\boldsymbol{\mathcal{R}} & -\boldsymbol{\mathcal{S}}\end{pmatrix}\begin{bmatrix}\mathbf{Q}\\ \mathbf{P}\end{bmatrix} + \begin{bmatrix}\boldsymbol{\mathcal{E}}\\ -\boldsymbol{\mathcal{F}}\end{bmatrix}. \tag{16}$$

Quantities $\mathbf{Q}$ and $\mathbf{P}$ in eq. (16) are 3×1 matrices describing absolute or relative changes of the position and slowness vectors calculated in ray tracing system (14). Quantities $\boldsymbol{\mathcal{R}}$, $\boldsymbol{\mathcal{S}}$ and $\boldsymbol{\mathcal{T}}$ on the right-hand side of eq. (16) are 3×3 coefficient matrices with elements

$$\mathcal{R}_{ij} = \frac{1}{2}\frac{\partial^2 G^{(x)}}{\partial x_i \partial x_j}, \qquad \mathcal{S}_{ij} = \frac{1}{2}\frac{\partial^2 G^{(x)}}{\partial x_i \partial p_j^{(x)}}, \qquad \mathcal{T}_{ij} = \frac{1}{2}\frac{\partial^2 G^{(x)}}{\partial p_i^{(x)} \partial p_j^{(x)}}. \tag{17}$$

Quantities $\boldsymbol{\mathcal{E}}$ and $\boldsymbol{\mathcal{F}}$ are 3×1 coefficient matrices. The definitions of $\boldsymbol{\mathcal{E}}$ and $\boldsymbol{\mathcal{F}}$ are context-dependent, that is, they depend on the specification of matrices $\mathbf{Q}$ and $\mathbf{P}$. Below we discuss some common specifications of matrices $\mathbf{Q}$, $\mathbf{P}$, $\boldsymbol{\mathcal{E}}$ and $\boldsymbol{\mathcal{F}}$.

One possibility is to define the components of the 3×1 matrices $\mathbf{Q}$ and $\mathbf{P}$ as partial derivatives,

$$Q_i = \frac{\partial x_i}{\partial \chi}, \qquad P_i = \frac{\partial p_i^{(x)}}{\partial \chi}, \tag{18}$$

where χ is an arbitrary parameter. We consider two specific options for parameter χ. The first option is to let $\chi = \gamma_1$ or $\chi = \gamma_2$ while the remaining ray coordinates are kept constant. In this case the model is assumed to be fixed, and coefficient matrices $\boldsymbol{\mathcal{E}}$ and $\boldsymbol{\mathcal{F}}$ are set equal to zero. The dynamic ray tracing equations are homogeneous in this case. The second option is to let χ be one of the model parameters, m, that is, we specify $\chi = m$. In this situation all three ray coordinates are constant, and matrices $\boldsymbol{\mathcal{E}}$ and $\boldsymbol{\mathcal{F}}$ are defined as

$$\mathcal{E}_i = \frac{1}{2}\frac{\partial^2 G^{(x)}}{\partial p_i^{(x)} \partial \chi}, \qquad \mathcal{F}_i = \frac{1}{2}\frac{\partial^2 G^{(x)}}{\partial x_i \partial \chi}. \tag{19}$$

In eq. (19), the differentiation is subject to the requirement that quantities x_i, $p_i^{(x)}$ and $\chi = m$ are independent variables.

As an alternative to defining $\mathbf{Q}$ and $\mathbf{P}$ by the partial derivatives in eq. (18) one may specify them as perturbations Δx_i and $\Delta p_i^{(x)}$,

$$Q_i = \Delta x_i, \qquad P_i = \Delta p_i^{(x)}. \tag{20}$$

These perturbations can be defined in various ways and, as above, we limit ourselves to two options. The first option is to let $\Delta\mathbf{x}$ and $\Delta\mathbf{p}^{(x)}$ denote the differences in the position and slowness vectors between the current ray (central ray) and a neighbouring ray (paraxial ray), for a given traveltime, τ, on the current ray. The medium parameters are assumed to be fixed, and matrices $\boldsymbol{\mathcal{E}}$ and $\boldsymbol{\mathcal{F}}$ are zero. As the second option, we require $\Delta\mathbf{x}$ and $\Delta\mathbf{p}^{(x)}$ to be the changes in the position and slowness vectors resulting from the perturbation of the model. Perturbations $\Delta\mathbf{x}$ and $\Delta\mathbf{p}^{(x)}$ are performed under the condition that the three ray coordinates are constant, and that matrices $\boldsymbol{\mathcal{E}}$ and $\boldsymbol{\mathcal{F}}$ are defined as:

$$\mathcal{E}_i = \frac{1}{2}\frac{\partial \Delta G^{(x)}}{\partial p_i^{(x)}}, \qquad \mathcal{F}_i = \frac{1}{2}\frac{\partial \Delta G^{(x)}}{\partial x_i}. \tag{21}$$

The perturbation $\Delta G^{(x)}$ in eq. (21) is performed under the condition that vectors $\mathbf{x}$ and $\mathbf{p}^{(x)}$ are fixed. Assuming perturbations of first order and using eqs (9) and (10), we can, therefore, express $\Delta G^{(x)}$ as:

$$\Delta G^{(x)} = \Delta a_{ijkl}^{(x)}(\mathbf{x})\, p_j^{(x)} p_l^{(x)} g_i^{(x)} g_k^{(x)}. \tag{22}$$

An important comment to the ray tracing equations (14) and inhomogeneous dynamic ray tracing equations (16). We emphasize that the numerical integration of these equations is performed in Cartesian coordinates. However, we shall show below that it is very useful to express the coefficients on the right-hand sides of these equations in terms of corresponding coefficients that are functions of the slowness vector in the curvilinear coordinate system.

5 SLOWNESS VECTOR AND ITS DERIVATIVES IN CURVILINEAR COORDINATES

In this section, we consider the slowness vector $\mathbf{p}^{(\xi)}$ given in curvilinear coordinates. In particular, we provide expressions for the first and second derivatives of $\mathbf{p}^{(\xi)}$ with respect to position coordinates x_i and slowness vector components $p_i^{(x)}$ in the Cartesian coordinate system.

Eq. (2) for the slowness vector in curvilinear coordinates yields the transformations

$$p_i^{(\xi)} = \frac{\partial x_j}{\partial \xi_i}\frac{\partial \tau}{\partial x_j} = H_{ji} p_j^{(x)}, \tag{23}$$

$$p_i^{(x)} = \frac{\partial \xi_j}{\partial x_i}\frac{\partial \tau}{\partial \xi_j} = \bar{H}_{ji} p_j^{(\xi)}. \tag{24}$$

Provided that position vector $\mathbf{x}$ and slowness vector $\mathbf{p}^{(x)}$ in Cartesian coordinates are independent quantities, differentiation of $p_i^{(x)}$ in eq. (24) with respect to x_k yields

$$\frac{\partial^2 \xi_j}{\partial x_k \partial x_i} p_j^{(\xi)} + \frac{\partial \xi_j}{\partial x_i}\frac{\partial \xi_l}{\partial x_k}\frac{\partial p_j^{(\xi)}}{\partial \xi_l} = 0. \tag{25}$$

Using eq. (4), its derivative with respect to x_k, and eq. (23) in eq. (25), we arrive at

$$\frac{\partial p_n^{(\xi)}}{\partial \xi_m} = H_{km}\bar{H}_{ji}\frac{\partial H_{in}}{\partial x_k} p_j^{(\xi)} = H_{km}\frac{\partial H_{in}}{\partial x_k} p_i^{(x)}. \tag{26}$$

An important observation that can be made from eq. (26) is that, generally, position vector $\boldsymbol{\xi}$ and slowness vector $\mathbf{p}^{(\xi)}$ are not independent. Eq. (26) shows that the two vectors become independent if, for example, $\partial H_{in}/\partial x_k = 0$. Because the $\boldsymbol{\xi}$ coordinates are orthogonal, the condition $\partial H_{in}/\partial x_k = 0$ implies that the $\boldsymbol{\xi}$ coordinates are Cartesian. Note also that, since the order of differentiation in the second-order derivative $\partial^2 \xi_j/\partial x_k \partial x_i$ is arbitrary, the differentiation of matrix $\bar{\mathbf{H}}$ satisfies

$$\frac{\partial \bar{H}_{jk}}{\partial x_i} = \frac{\partial \bar{H}_{ji}}{\partial x_k}. \tag{27}$$

Applying eq. (6) in eq. (27) yields a corresponding relation involving matrix $\mathbf{H}$:

$$\frac{\partial H_{kj}}{\partial x_i} = \frac{\partial H_{ij}}{\partial x_k}. \tag{28}$$

Since the position and slowness vectors in curvilinear coordinates are generally not independent, it is necessary to express slowness vector $\mathbf{p}^{(\xi)}$ as a function of the Cartesian phase-space coordinates $[\mathbf{x}, \mathbf{p}^{(x)}]$. With this in view, we define a 3×3 matrix $\mathbf{K}$ with elements

$$K_{ij} = \frac{\partial p_j^{(\xi)}}{\partial x_i}. \tag{29}$$

Considering $\mathbf{p}^{(\xi)}$ as a function of Cartesian phase-space coordinates $\mathbf{x}, \mathbf{p}^{(x)}$, and taking into account eq. (23), we obtain the first- and second-order derivatives of $\mathbf{p}^{(\xi)}$:

$$\frac{\partial p_k^{(\xi)}}{\partial x_m} = K_{mk} = \frac{\partial H_{ik}}{\partial x_m} p_i^{(x)}, \tag{30}$$

$$\frac{\partial p_k^{(\xi)}}{\partial p_m^{(x)}} = H_{mk}, \tag{31}$$

$$\frac{\partial^2 p_k^{(\xi)}}{\partial x_n \partial x_m} = \frac{\partial^2 H_{ik}}{\partial x_n \partial x_m} p_i^{(x)}, \tag{32}$$

$$\frac{\partial^2 p_k^{(\xi)}}{\partial x_n \partial p_m^{(x)}} = \frac{\partial H_{mk}}{\partial x_n}, \tag{33}$$

$$\frac{\partial^2 p_k^{(\xi)}}{\partial p_n^{(x)} \partial p_m^{(x)}} = 0. \tag{34}$$

6 DERIVATIVES OF EIGENVALUES OF THE CHRISTOFFEL MATRIX IN A MIXED PHASE-SPACE DOMAIN

For curvilinear coordinates one can write expressions completely analogous to eqs (12) and (13), relating quantities $\boldsymbol{\xi}$, $\mathbf{p}^{(\xi)}$, $\mathcal{H}^{(\xi)}$ and $G^{(\xi)}$. Eigenvalue $G^{(\xi)}$ is required to satisfy the eikonal equation

$$G^{(\xi)} = 1. \tag{35}$$

The following considerations simplify considerably if they are performed in a mixed phase-space domain, formed by the Cartesian position vector $\mathbf{x}$ and slowness vector $\mathbf{p}^{(\xi)}$ in curvilinear coordinates. All quantities related to this domain are denoted by symbol $\mathcal{M}$. In these mixed phase-space coordinates, we express the Christoffel matrix and any of its eigenvalues as

$$\Gamma_{ik}^{\mathcal{M}}\left[\mathbf{x}, \mathbf{p}^{(\xi)}\right] = a_{ijkl}^{(\xi)}(\mathbf{x}) p_j^{(\xi)} p_l^{(\xi)}, \tag{36}$$

$$G^{\mathcal{M}}\left[\mathbf{x}, \mathbf{p}^{(\xi)}\right] = \Gamma_{ik}^{\mathcal{M}}\left[\mathbf{x}, \mathbf{p}^{(\xi)}\right] g_i^{\mathcal{M}}\left[\mathbf{x}, \mathbf{p}^{(\xi)}\right] g_k^{\mathcal{M}}\left[\mathbf{x}, \mathbf{p}^{(\xi)}\right]. \tag{37}$$

Here, vector $\mathbf{g}^{\mathcal{M}}$ equals the eigenvector $\mathbf{g}^{(\xi)}$ in curvilinear coordinates. If the traveltime is the variable along rays, we specify the Hamiltonian function in mixed phase-space coordinates as

$$\mathcal{H}^{\mathcal{M}}\left[\mathbf{x}, \mathbf{p}^{(\xi)}\right] = \frac{1}{2}\left\{G^{\mathcal{M}}\left[\mathbf{x}, \mathbf{p}^{(\xi)}\right] - 1\right\}. \tag{38}$$

Given that $\mathbf{x}$ and $\boldsymbol{\xi}$ correspond to the same location, we evidently have

$$G^{(x)}\left[\mathbf{x}, \mathbf{p}^{(x)}\right] = G^{\mathcal{M}}\left[\mathbf{x}, \mathbf{p}^{(\xi)}\right] = G^{(\xi)}\left[\boldsymbol{\xi}, \mathbf{p}^{(\xi)}\right]. \tag{39}$$

Along a ray, $G^{(x)} = G^{\mathcal{M}} = G^{(\xi)} = 1$. Differentiation of eq. (39) with respect to x_m and $p_m^{(x)}$ yields:

$$\frac{\partial G^{(x)}}{\partial x_m} = \frac{\partial G^{\mathcal{M}}}{\partial x_m} + \frac{\partial G^{\mathcal{M}}}{\partial p_k^{(\xi)}}\frac{\partial p_k^{(\xi)}}{\partial x_m}, \tag{40}$$

$$\frac{\partial G^{(x)}}{\partial p_m^{(x)}} = \frac{\partial G^{\mathcal{M}}}{\partial p_k^{(\xi)}}\frac{\partial p_k^{(\xi)}}{\partial p_m^{(x)}}. \tag{41}$$

The derivatives $\partial p_k^{(\xi)}/\partial x_m$ and $\partial p_k^{(\xi)}/\partial p_m^{(x)}$ are given by eqs (30) and (31), respectively.

In Cartesian coordinates, the ray velocity vector $\mathbf{v}^{(x)}$ and the eta vector $\boldsymbol{\eta}^{(x)}$ are given by eq. (15). In curvilinear coordinates we define:

$$v_m^{(\xi)} = \frac{1}{2}\frac{\partial G^{(\xi)}}{\partial p_m^{(\xi)}}, \qquad \eta_m^{(\xi)} = -\frac{1}{2}\frac{\partial G^{(\xi)}}{\partial \xi_m}, \tag{42}$$

and in mixed phase-space coordinates $[\mathbf{x}, \mathbf{p}^{(\xi)}]$, we define

$$v_m^{\mathcal{M}} = \frac{1}{2}\frac{\partial G^{\mathcal{M}}}{\partial p_m^{(\xi)}}, \qquad \eta_m^{\mathcal{M}} = -\frac{1}{2}\frac{\partial G^{\mathcal{M}}}{\partial x_m}. \tag{43}$$

Here the two differentiations have been performed for fixed vectors $\mathbf{x}$ and $\mathbf{p}^{(\xi)}$, respectively. It follows from eqs (40), (42) and (43) that the components of vectors $\mathbf{v}^{\mathcal{M}}$ and $\boldsymbol{\eta}^{\mathcal{M}}$ are given by

$$v_m^{\mathcal{M}} = v_m^{(\xi)}, \qquad \eta_m^{\mathcal{M}} = \eta_m^{(x)0}, \tag{44}$$

where $\boldsymbol{\eta}^{(x)0}$ is the eta vector in Cartesian coordinates obtained by ignoring the variation of matrix $\mathbf{H}$ with $\mathbf{x}$ (Iversen & Pšenčík 2007).

Further differentiation of eqs (40) and (41) yields the second-order derivatives:

$$\frac{\partial^2 G^{(x)}}{\partial x_n x_m} = \frac{\partial^2 G^{\mathcal{M}}}{\partial x_n \partial x_m} + \frac{\partial^2 G^{\mathcal{M}}}{\partial x_n \partial p_k^{(\xi)}}\frac{\partial p_k^{(\xi)}}{\partial x_m} + \frac{\partial^2 G^{\mathcal{M}}}{\partial x_m \partial p_l^{(\xi)}}\frac{\partial p_l^{(\xi)}}{\partial x_n} + \frac{\partial^2 G^{\mathcal{M}}}{\partial p_l^{(\xi)} \partial p_k^{(\xi)}}\frac{\partial p_l^{(\xi)}}{\partial x_n}\frac{\partial p_k^{(\xi)}}{\partial x_m} + \frac{\partial G^{\mathcal{M}}}{\partial p_k^{(\xi)}}\frac{\partial^2 p_k^{(\xi)}}{\partial x_n \partial x_m}, \tag{45}$$

$$\frac{\partial^2 G^{(x)}}{\partial x_n \partial p_m^{(x)}} = \frac{\partial^2 G^{\mathcal{M}}}{\partial x_n \partial p_k^{(\xi)}}\frac{\partial p_k^{(\xi)}}{\partial p_m^{(x)}} + \frac{\partial^2 G^{\mathcal{M}}}{\partial p_l^{(\xi)} \partial p_k^{(\xi)}}\frac{\partial p_l^{(\xi)}}{\partial x_n}\frac{\partial p_k^{(\xi)}}{\partial p_m^{(x)}} + \frac{\partial G^{\mathcal{M}}}{\partial p_k^{(\xi)}}\frac{\partial^2 p_k^{(\xi)}}{\partial x_n \partial p_m^{(x)}}, \tag{46}$$

$$\frac{\partial^2 G^{(x)}}{\partial p_n^{(x)} \partial p_m^{(x)}} = \frac{\partial^2 G^{\mathcal{M}}}{\partial p_l^{(\xi)} \partial p_k^{(\xi)}}\frac{\partial p_l^{(\xi)}}{\partial p_n^{(x)}}\frac{\partial p_k^{(\xi)}}{\partial p_m^{(x)}}. \tag{47}$$

Here, derivatives $\partial^2 p_k^{(\xi)}/\partial x_n \partial x_m$ and $\partial^2 p_k^{(\xi)}/\partial x_n \partial p_m^{(x)}$ are given by eqs (32) and (33), respectively. In deriving eq. (47), we used eq. (34).

Let us now consider the terms given by eq. (19). Mixed double differentiation of eigenvalue $G^{(x)}$ with respect to the arbitrary parameter χ, introduced in eq. (18), as well as with respect to one of the phase-space coordinates, x_m or $p_m^{(x)}$, yields:

$$\frac{\partial^2 G^{(x)}}{\partial x_m \partial \chi} = \frac{\partial^2 G^{\mathcal{M}}}{\partial x_m \partial \chi} + \frac{\partial^2 G^{\mathcal{M}}}{\partial p_k^{(\xi)} \partial \chi}\frac{\partial p_k^{(\xi)}}{\partial x_m}, \tag{48}$$

$$\frac{\partial^2 G^{(x)}}{\partial p_m^{(x)} \partial \chi} = \frac{\partial^2 G^{\mathcal{M}}}{\partial p_k^{(\xi)} \partial \chi}\frac{\partial p_k^{(\xi)}}{\partial p_m^{(x)}}. \tag{49}$$

Likewise, we find that the terms in eq. (21) can be expressed as:

$$\frac{\partial \Delta G^{(x)}}{\partial x_m} = \frac{\partial \Delta G^{\mathcal{M}}}{\partial x_m} + \frac{\partial \Delta G^{\mathcal{M}}}{\partial p_k^{(\xi)}}\frac{\partial p_k^{(\xi)}}{\partial x_m}, \tag{50}$$

$$\frac{\partial \Delta G^{(x)}}{\partial p_m^{(x)}} = \frac{\partial \Delta G^{\mathcal{M}}}{\partial p_k^{(\xi)}}\frac{\partial p_k^{(\xi)}}{\partial p_m^{(x)}}. \tag{51}$$

7 TRANSFORMATION RELATIONS FOR COEFFICIENTS OF THE DIFFERENTIAL EQUATIONS

The numerical integration of ray tracing equations (14) and inhomogeneous dynamic ray tracing equations (16) is performed in Cartesian coordinates. The purpose of this section is to relate the coefficients forming the right-hand sides of these equations to corresponding coefficients

belonging to the mixed phase-space domain. We recall that the latter domain is formed by the Cartesian position vector $\mathbf{x}$ and slowness vector $\mathbf{p}^{(\xi)}$ in curvilinear coordinates.

Eqs (29), (31) and (40)–(43) yield:

$$v_m^{(x)} = H_{mk} v_k^{\mathcal{M}}, \qquad \eta_m^{(x)} = \eta_m^{\mathcal{M}} - K_{mk} v_k^{\mathcal{M}}, \tag{52}$$

or in vectorial form:

$$\mathbf{v}^{(x)} = \mathbf{H}\mathbf{v}^{\mathcal{M}}, \qquad \boldsymbol{\eta}^{(x)} = \boldsymbol{\eta}^{\mathcal{M}} - \mathbf{K}\mathbf{v}^{\mathcal{M}}. \tag{53}$$

In this way, we establish a transformation equation for the coefficients of ray tracing equations (14),

$$\begin{pmatrix} \mathbf{v}^{(x)} \\ \boldsymbol{\eta}^{(x)} \end{pmatrix} = \mathbf{C} \begin{pmatrix} \mathbf{v}^{\mathcal{M}} \\ \boldsymbol{\eta}^{\mathcal{M}} \end{pmatrix}, \tag{54}$$

which also introduces the 6×6 matrix

$$\mathbf{C} = \begin{pmatrix} \mathbf{H} & \mathbf{0} \\ -\mathbf{K} & \mathbf{I} \end{pmatrix}. \tag{55}$$

Let us define

$$\mathcal{R}_{nm}^{\mathcal{M}} = \frac{1}{2} \frac{\partial^2 G^{\mathcal{M}}}{\partial x_n x_m}, \qquad \mathcal{S}_{nk}^{\mathcal{M}} = \frac{1}{2} \frac{\partial^2 G^{\mathcal{M}}}{\partial x_n p_k^{(\xi)}}, \qquad \mathcal{T}_{lk}^{\mathcal{M}} = \frac{1}{2} \frac{\partial^2 G^{\mathcal{M}}}{\partial p_l^{(\xi)} p_k^{(\xi)}}, \tag{56}$$

$$U_{nm} = \frac{1}{2} \frac{\partial G^{\mathcal{M}}}{\partial p_k^{(\xi)}} \frac{\partial^2 p_k^{(\xi)}}{\partial x_n \partial x_m}, \qquad V_{nm} = \frac{1}{2} \frac{\partial G^{\mathcal{M}}}{\partial p_k^{(\xi)}} \frac{\partial^2 p_k^{(\xi)}}{\partial x_n \partial p_m^{(x)}}. \tag{57}$$

Applying relations (29), (31) and (56), (57), we can rewrite eqs (45)–(47) to read:

$$\mathcal{R}_{nm} = \mathcal{R}_{nm}^{\mathcal{M}} + \mathcal{S}_{nk}^{\mathcal{M}} K_{mk} + \mathcal{S}_{ml}^{\mathcal{M}} K_{nl} + \mathcal{T}_{lk}^{\mathcal{M}} K_{nl} K_{mk} + U_{nm}, \tag{58}$$

$$\mathcal{S}_{nm} = \mathcal{S}_{nk}^{\mathcal{M}} H_{mk} + \mathcal{T}_{lk}^{\mathcal{M}} K_{nl} H_{mk} + V_{nm}, \tag{59}$$

$$\mathcal{T}_{nm} = \mathcal{T}_{lk}^{\mathcal{M}} H_{nl} H_{mk}, \tag{60}$$

Using matrix form, eqs (58)–(60) can be expressed in a single matrix transformation equation for the coefficients of the dynamic ray tracing system (16),

$$\begin{pmatrix} \boldsymbol{\mathcal{S}}^T & \boldsymbol{\mathcal{T}} \\ -\boldsymbol{\mathcal{R}} & -\boldsymbol{\mathcal{S}} \end{pmatrix} = \mathbf{C} \begin{pmatrix} \boldsymbol{\mathcal{S}}^{\mathcal{M}\,T} & \boldsymbol{\mathcal{T}}^{\mathcal{M}} \\ -\boldsymbol{\mathcal{R}}^{\mathcal{M}} & -\boldsymbol{\mathcal{S}}^{\mathcal{M}} \end{pmatrix} \mathbf{D} + \begin{pmatrix} \mathbf{V}^T & \mathbf{0} \\ -\mathbf{U} & -\mathbf{V} \end{pmatrix}. \tag{61}$$

Here matrix $\mathbf{C}$ is defined in eq. (55) and $\mathbf{D}$ is the 6×6 matrix

$$\mathbf{D} = \begin{pmatrix} \mathbf{I} & \mathbf{0} \\ \mathbf{K}^T & \mathbf{H}^T \end{pmatrix}. \tag{62}$$

Considering eqs (19)–(21) and (48)–(51) we find the following matrix equation for the coefficients $\boldsymbol{\mathcal{E}}$ and $\boldsymbol{\mathcal{F}}$ of the dynamic ray tracing system (16):

$$\begin{pmatrix} \boldsymbol{\mathcal{E}} \\ -\boldsymbol{\mathcal{F}} \end{pmatrix} = \mathbf{C} \begin{pmatrix} \boldsymbol{\mathcal{E}}^{\mathcal{M}} \\ -\boldsymbol{\mathcal{F}}^{\mathcal{M}} \end{pmatrix}. \tag{63}$$

8 PROPERTIES OF TRANSFORMED COEFFICIENTS

In this section, we discuss the meaning of selected coefficients in the transformation eqs (54) and (61). Particular attention is given to the isotropic case and other cases where the ray velocity and slowness vectors are parallel. In the isotropic case, one will expect the transformations derived in eqs (54) and (61) to reduce to trivial relations, regardless of the values of first- and second-order derivatives of matrix $\mathbf{H}$.

8.1 Vector η

One can express eq. (52) in alternative forms:

$$\eta_m^{(x)} = \eta_m^{\mathcal{M}} - \frac{\partial H_{ik}}{\partial x_m} H_{jk} v_j^{(x)} p_i^{(x)}, \tag{64}$$

$$\eta_m^{(x)} = \eta_m^{\mathcal{M}} - \frac{\partial H_{ij}}{\partial x_m} H_{ik} v_j^{(\xi)} p_k^{(\xi)}. \tag{65}$$

Also, one can observe that vector $\boldsymbol{\eta}^{\mathcal{M}}$ is related to vector $\boldsymbol{\eta}^{(\xi)}$ via the transformation

$$\eta_m^{\mathcal{M}} = H_{mj}\eta_j^{(\xi)}. \tag{66}$$

In view of eq. (4), it is clear that tensor $H_{jk}\,\partial H_{ik}/\partial x_m$ is antisymmetric with respect to indices i and j. This allows the following rewrite of eq. (64):

$$\eta_m^{(x)} = \eta_m^{\mathcal{M}} - \frac{1}{2}\frac{\partial H_{ik}}{\partial x_m}H_{jk}\big[v_j^{(x)}p_i^{(x)} - v_i^{(x)}p_j^{(x)}\big]. \tag{67}$$

The factor $[v_j^{(x)}p_i^{(x)} - v_i^{(x)}p_j^{(x)}]$ in eq. (67) is a component of cross product $\mathbf{v}^{(x)} \times \mathbf{p}^{(x)}$. In all situations where the ray velocity vector is parallel to the slowness vector, this cross-product is zero and eq. (67) thus reduces to:

$$\eta_m^{(x)} = \eta_m^{\mathcal{M}} = H_{mj}\eta_j^{(\xi)}. \tag{68}$$

Eq. (68) is always satisfied in an isotropic medium. In an anisotropic medium, where matrix $\mathbf{H}$ varies with position $\mathbf{x}$, eq. (68) is only satisfied in specific situations, in which $\mathbf{v}^{(x)} \parallel \mathbf{p}^{(x)}$.

8.2 Matrix $\mathbf{S}^{\mathcal{M}}$

Eq. (59) can be altered to read:

$$\mathcal{S}_{nm} = \mathcal{S}_{nk}^{\mathcal{M}}H_{mk} + \frac{\partial H_{ij}}{\partial x_n}H_{kj}\big[v_k^{(x)}\delta_{im} - p_k^{(x)}\mathcal{T}_{im}\big]. \tag{69}$$

If $\mathbf{v}^{(x)} \parallel \mathbf{p}^{(x)}$, we have $v_k^{(x)} = v^2 p_k^{(x)}$, where v is the ray velocity: the length of vector $\mathbf{v}^{(x)}$, which is equal to the phase velocity in this case. Inserting this in eq. (69) we get:

$$\mathcal{S}_{nm} = \mathcal{S}_{nk}^{\mathcal{M}}H_{mk} + \frac{\partial H_{ij}}{\partial x_n}H_{kj}p_k^{(x)}\big(v^2\delta_{im} - \mathcal{T}_{im}\big). \tag{70}$$

The second term on the right-hand side of eq. (70) is generally not zero in an anisotropic medium. In an isotropic medium, however,

$$\mathcal{T}_{im} = v^2\delta_{im}, \tag{71}$$

and thus

$$\mathcal{S}_{nm} = \mathcal{S}_{nk}^{\mathcal{M}}H_{mk}. \tag{72}$$

8.3 Matrix $\mathbf{R}^{\mathcal{M}}$

Consider eq. (58), which can be altered to read:

$$\mathcal{R}_{nm} = \mathcal{R}_{nm}^{\mathcal{M}} + \mathcal{S}_{nk}^{\mathcal{M}}K_{mk} + \mathcal{S}_{ml}^{\mathcal{M}}K_{nl} + \mathcal{T}_{lk}^{\mathcal{M}}\frac{\partial H_{ik}}{\partial x_m}\frac{\partial H_{jl}}{\partial x_n}p_i^{(x)}p_j^{(x)} + H_{jk}\frac{\partial^2 H_{ik}}{\partial x_n \partial x_m}p_i^{(x)}v_j^{(x)}. \tag{73}$$

Assuming $\mathbf{v}^{(x)} \parallel \mathbf{p}^{(x)}$, which implies $v_k^{(x)} = v^2 p_k^{(x)}$, we can express eq. (73) as:

$$\mathcal{R}_{nm} = \mathcal{R}_{nm}^{\mathcal{M}} + \mathcal{S}_{nk}^{\mathcal{M}}K_{mk} + \mathcal{S}_{ml}^{\mathcal{M}}K_{nl} + \left[\left(\mathcal{T}_{lk}^{\mathcal{M}} - v^2\delta_{lk}\right)\frac{\partial H_{ik}}{\partial x_m}\frac{\partial H_{jl}}{\partial x_n} + v^2\frac{\partial}{\partial x_n}\left(H_{jk}\frac{\partial H_{ik}}{\partial x_m}\right)\right]p_i^{(x)}p_j^{(x)}. \tag{74}$$

Based on eq. (4), it can be concluded that tensor $\partial(H_{jk}\,\partial H_{ik}/\partial x_m)/\partial x_n$ is antisymmetric with respect to indices i and j. As a result, the corresponding term in eq. (74) is zero. Moreover, if the medium is isotropic, the term including the expression $(\mathcal{T}_{lk}^{\mathcal{M}} - v^2\delta_{lk})$ is also zero since $\mathcal{T}_{lk}^{\mathcal{M}} = v^2\delta_{lk}$. In the isotropic case it remains to see what happens to the two terms (of the same form) including $\mathcal{S}_{nk}^{\mathcal{M}}$. Since tensor $H_{ik}\,\partial H_{jk}/\partial x_m$ is antisymmetric in indices i and j, we arrive at:

$$\mathcal{S}_{nk}^{\mathcal{M}}K_{mk} = 2v\frac{\partial v}{\partial x_n}H_{ik}\frac{\partial H_{jk}}{\partial x_m}p_i^{(x)}p_j^{(x)} = 0. \tag{75}$$

To derive eq. (75), we used eqs (17), (72) and the eikonal equation (11) specified for the isotropic case, $G^{(x)} = v^2 p_l^{(x)}p_l^{(x)}$. As a consequence, in an isotropic medium eq. (74) reduces to

$$\mathcal{R}_{nm} = \mathcal{R}_{nm}^{\mathcal{M}}. \tag{76}$$

9 COMPUTATIONAL PROCEDURE

To perform ray tracing and dynamic ray tracing in an anisotropic medium whose symmetry system varies continuously, we solve eqs (14) and (16) numerically. Transformation relation (54) is used to compute the right-hand sides of eq. (14). To compute the right-hand sides of eq. (16), one can use the relevant transformations given by eqs (61) and (63).

Using eq. (54), we obtain vectors $\mathbf{v}^{(x)}$ and $\boldsymbol{\eta}^{(x)}$ from vectors $\mathbf{v}^{\mathcal{M}}$ and $\boldsymbol{\eta}^{\mathcal{M}}$, which, in turn, are computed from $\mathbf{p}^{(\xi)}$, $a^{(\xi)}_{ijkl}(\mathbf{x})$ and $[\partial a^{(\xi)}_{ijkl}/\partial x_m](\mathbf{x})$. The latter quantities are used in expressions (43), which must be specified for the considered type of anisotropy and in curvilinear coordinates (this means that, e.g. in the case of *P*-wave ray tracing for a TI medium, the right-hand sides of eq. (43) depend on only four effective elastic parameters).

Eq. (61) transforms matrices $\boldsymbol{\mathcal{R}}^{\mathcal{M}}$, $\boldsymbol{\mathcal{S}}^{\mathcal{M}}$ and $\boldsymbol{\mathcal{T}}^{\mathcal{M}}$ to the corresponding matrices $\boldsymbol{\mathcal{R}}$, $\boldsymbol{\mathcal{S}}$ and $\boldsymbol{\mathcal{T}}$. The computation of matrices $\boldsymbol{\mathcal{R}}^{\mathcal{M}}$, $\boldsymbol{\mathcal{S}}^{\mathcal{M}}$ and $\boldsymbol{\mathcal{T}}^{\mathcal{M}}$ requires quantities $\mathbf{p}^{(\xi)}$, $a^{(\xi)}_{ijkl}(\mathbf{x})$, $[\partial a^{(\xi)}_{ijkl}/\partial x_m](\mathbf{x})$, and $[\partial^2 a^{(\xi)}_{ijkl}/\partial x_n \partial x_m](\mathbf{x})$. These quantities are used in expressions (56), specified again for the considered type of symmetry. The matrices $\mathbf{U}$ and $\mathbf{V}$ in eq. (61) are calculated using eq. (57) with (32) and (33). Finally, eq. (63) transforms quantities $\boldsymbol{\mathcal{E}}^{\mathcal{M}}$, $\boldsymbol{\mathcal{F}}^{\mathcal{M}}$ to $\boldsymbol{\mathcal{E}}$, $\boldsymbol{\mathcal{F}}$. The computation of matrices $\boldsymbol{\mathcal{E}}^{\mathcal{M}}$ and $\boldsymbol{\mathcal{F}}^{\mathcal{M}}$ requires quantities $\mathbf{p}^{(\xi)}$ and $a^{(\xi)}_{ijkl}(\mathbf{x})$, which also appear in expressions (58), specified for the considered anisotropy.

The initialization of the numerical integration of eqs (14) and (16) requires the specification of $\mathbf{x}$, $\mathbf{p}^{(x)}$, $\mathbf{Q}$ and $\mathbf{P}$ at an initial point. The basic step in the specification of the above quantities is determination of slowness vector $\mathbf{p}^{(x)}$. It is specified by unit vector $\mathbf{n}^{(x)}$, perpendicular to the wave front at the initial point and specified in Cartesian coordinates. Unit vector $\mathbf{n}^{(x)}$ must be transformed into curvilinear coordinates, in which the corresponding phase velocity can be found, so that slowness vector $\mathbf{p}^{(\xi)}$ can be determined and subsequently transformed into $\mathbf{p}^{(x)}$. For more details see Iversen & Pšenčík (2007). A similar procedure is used to specify the initial values of $\mathbf{Q}$ and $\mathbf{P}$.

10 NUMERICAL EXAMPLES

We illustrate the accuracy of the proposed procedure on the models and configuration used by Iversen & Pšenčík (2007). In all examples, the depth axis, x_3, is positive down.

10.1 Models and configuration

Consider two smooth models of TI symmetry and one model of OR symmetry. The heterogeneity of the models is generated by the specification of elastic moduli $A^{(\xi)}_{\alpha\beta}$ and Euler angles λ, μ and ν [used for parametrizing matrix $\mathbf{H}$; eq. (8)] on two non-parallel isosurfaces. For points between these isosurfaces, the elastic moduli and the Euler angles are interpolated linearly in the vertical direction. The upper surface is a horizontal plane ($x_3 = 0$); the lower surface is slightly curved with maximum dip approximately along the line $x_2 = x_1$. Since the depth of the lower surface slightly varies around the depth of 2.5 km, the elastic moduli and Euler angles vary in the model not only vertically, but also slightly laterally. In this way, we can obtain $A^{(\xi)}_{\alpha\beta}(\mathbf{x})$, $\mathbf{H}(\mathbf{x})$ and their first- and second-order derivatives at every point $\mathbf{x}$.

First, we consider two models referred to as HTI_{FIX} and HTI_{ROT} whose anisotropy is of the HTI type, that is, a TI medium with a horizontal symmetry axis. For both models, the elastic moduli belonging to the curvilinear coordinate systems at the upper and lower isosurfaces are identical. At the upper surface the symmetric matrix of the density-normalized elastic moduli corresponding to a TI medium with a vertical axis of symmetry, measured in $(\mathrm{km\ s^{-1}})^2$, reads:

$$\begin{pmatrix} 15.71 & 5.05 & 4.46 & 0 & 0 & 0 \\ & 15.71 & 4.46 & 0 & 0 & 0 \\ & & 13.39 & 0 & 0 & 0 \\ & & & 4.98 & 0 & 0 \\ & & & & 4.98 & 0 \\ & & & & & 5.33 \end{pmatrix}.$$

At the lower surface, it reads:

$$\begin{pmatrix} 35.35 & 11.36 & 10.04 & 0 & 0 & 0 \\ & 35.35 & 10.04 & 0 & 0 & 0 \\ & & 30.13 & 0 & 0 & 0 \\ & & & 11.21 & 0 & 0 \\ & & & & 11.21 & 0 \\ & & & & & 11.99 \end{pmatrix}.$$

Models HTI_{FIX} and HTI_{ROT} differ in the way the curvilinear coordinate system is varied with respect to the Cartesian coordinate system. In model HTI_{FIX}, the symmetry axis is parallel to the x_1 axis on both isosurfaces; hence, the direction of the symmetry axis is fixed throughout the model. The angles parametrizing matrix $\mathbf{H}$ have the values $\lambda = 90^\circ$, $\mu = 0^\circ$ and $\nu = 0^\circ$ on both isosurfaces.

In model HTI_{ROT}, the symmetry axis is parallel to the x_1 axis along the lower isosurface, as in model HTI_{FIX}, but on the upper isosurface the symmetry axis makes an angle of 45° with the x_1 axis. We therefore, have a medium where the angle between the x_1 axis and the symmetry axis varies linearly from 45° to 0° along any vertical line between the upper and lower isosurface. Considering the definitions of angles λ, μ, ν, this situation corresponds to $\lambda = 90^\circ$, $\mu = -45^\circ$ and $\nu = 0^\circ$ on the upper isosurface and $\lambda = 90^\circ$, $\mu = 0^\circ$ and $\nu = 0^\circ$ on the lower isosurface.

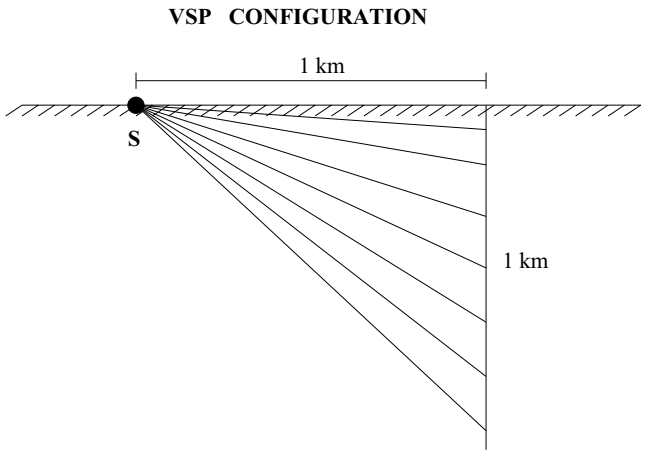

Figure 1. Schematic configuration of experiments.

In addition to the two HTI models, consider a third model, referred to as OR_{ROT}. The geometry of this model is exactly the same as that of the two HTI models, only now the density-normalized elastic moduli at the two isosurfaces correspond to OR symmetry. At the upper surface the matrix of the density-normalized elastic moduli, measured in $(\mathrm{km\ s^{-1}})^2$, reads:

$$\begin{pmatrix} 9.00 & 3.60 & 2.25 & 0 & 0 & 0 \\ & 9.84 & 2.40 & 0 & 0 & 0 \\ & & 5.94 & 0 & 0 & 0 \\ & & & 2.00 & 0 & 0 \\ & & & & 1.60 & 0 \\ & & & & & 2.18 \end{pmatrix}.$$

At the lower surface, it reads:

$$\begin{pmatrix} 19.80 & 7.92 & 4.95 & 0 & 0 & 0 \\ & 21.65 & 5.28 & 0 & 0 & 0 \\ & & 13.07 & 0 & 0 & 0 \\ & & & 4.40 & 0 & 0 \\ & & & & 3.52 & 0 \\ & & & & & 4.80 \end{pmatrix}.$$

The above moduli are almost identical to those used by Schoenberg & Helbig (1997). Compared to the HTI models, the specification of angles λ and ν is retained, but conversely to model HTI_{ROT}, angle μ takes the values 0° and -45° at the upper and lower isosurfaces, respectively.

Consider the VSP survey configuration shown in Fig. 1 with a source point located at the origin of the Cartesian coordinate system and a vertical receiver line, for which $x_1 = 1$ km and $x_2 = 0$ km. The receivers are distributed between depths $x_3 = 0.04$ km and $x_3 = 0.96$ km, with equidistant spacing 0.04 km. The rotation of the curvilinear coordinate system relative to the plane of the survey (the x_1– x_3 plane) for models HTI_{ROT} and OR_{ROT} is outlined in Fig. 2.

For each model described above, we performed two ray tracing and homogeneous dynamic ray tracing simulations for the direct *P* wave. The first computation was based on the use of the formulae proposed above and made use of the elastic moduli $A^{(\xi)}_{\alpha\beta}$, matrix **H**, and their first- and second-order derivatives with respect to coordinates x_i. The second, standard, computation, based on the use of the program package ANRAY (Gajewski & Pšenčík 1987), was performed in Cartesian coordinates. Before the latter type of computation, a model preparation step was needed for elastic moduli, consisting of transforming the elastic moduli in curvilinear coordinates, $A^{(\xi)}_{\alpha\beta}$, into a full set of 21 elastic moduli in Cartesian coordinates, $A^{(x)}_{\alpha\beta}$, using matrix **H**. This step was performed at each of the isosurfaces. To illustrate the typical behaviour of rays and traveltimes, see Fig. 3 corresponding to model HTI_{ROT}. We can see that the rays in this model are 3-D curves. Their slight deviation from the vertical plane is caused by the variation of the symmetry planes with depth, and also by the slight lateral heterogeneity of the model. Ray diagrams and traveltimes for the HTI_{ROT} model and the other two models can be found in Iversen & Pšenčík (2007).

In the following sections, we show relative differences of traveltime and geometrical spreading obtained with the procedure proposed in this paper and standard procedure (ANRAY) for the three above-described models. The traveltime results have been reported earlier by Iversen & Pšenčík (2007). They are also presented here to enable the comparison with results for geometrical spreading. Generally, spreading shows greater differences.

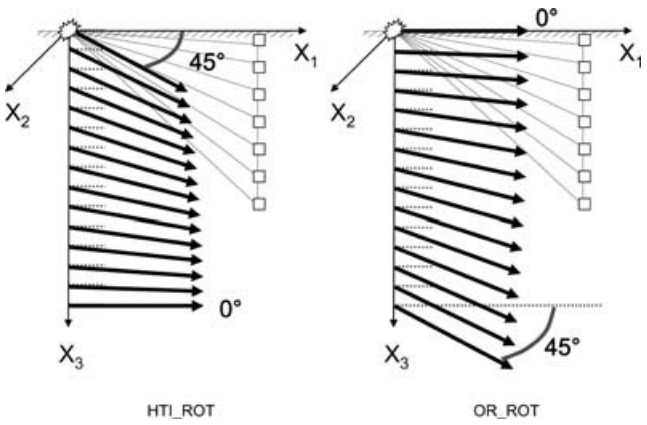

Figure 2. Cartoon illustrating the rotation of the curvilinear coordinates between the two isosurfaces in the models HTI_{ROT} (left-hand panel) and OR_{ROT} (right-hand panel).

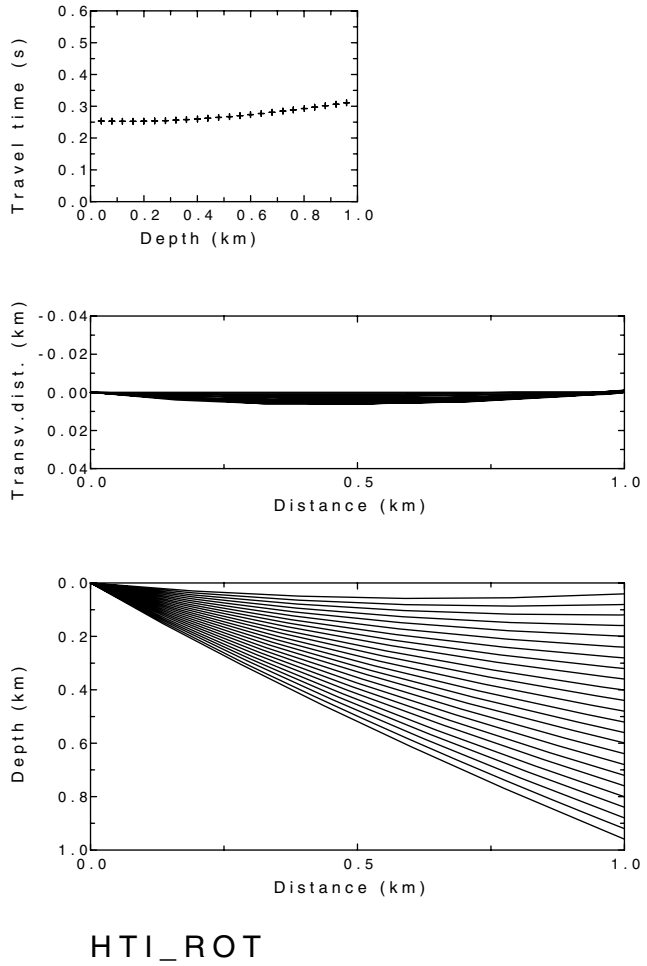

Figure 3. Results of standard ray tracing for model HTI_{ROT}. Top panel: Computed traveltimes. Middle panel: Projection of rays in model HTI_{ROT} into the horizontal plane. Bottom panel: Projection of rays in model HTI_{ROT} into the vertical plane.

10.2 Ray and dynamic ray tracing in model HTI_{FIX}

In model HTI_{FIX}, the linear interpolation of elastic moduli $A_{\alpha\beta}^{(\xi)}$ is perfectly consistent with the linear interpolation of rotated elastic moduli $A_{\alpha\beta}^{(x)}$. As a consequence, the traveltimes and the geometrical spreading values resulting from both computations should, in theory, be identical. This is confirmed in Fig. 4. The largest relative traveltime differences between the two computations are about 0.03 per cent. The differences for the geometrical spreading are even smaller.

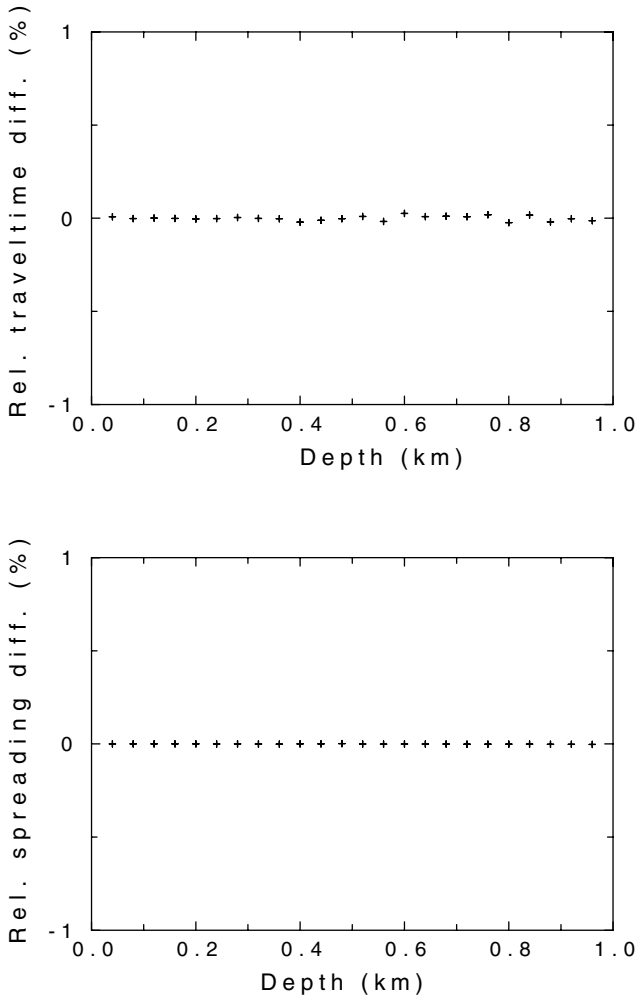

Figure 4. Relative differences in traveltime and geometrical spreading (in per cent) for the procedure proposed above and for the standard procedure, using model HTI_{FIX}.

10.3 Ray and dynamic ray tracing in model HTI_{ROT}

If the symmetry axes at the upper and lower isosurfaces are not parallel, the linear interpolation of the transformed elastic moduli $A_{\alpha\beta}^{(x)}$ yields values which are generally different from the values obtained by linear interpolation of elastic moduli $A_{\alpha\beta}^{(\xi)}$. The interpolated values of $A_{\alpha\beta}^{(x)}$ become inconsistent with the TI symmetry. Thus, the two computations yield slightly different values of the elastic moduli at the locations between the two isosurfaces. This, in the end, leads to different ray traveltimes and geometrical spreading values, see Fig. 5. The largest relative difference in traveltime is now about 0.37 per cent, and the relative differences in the spreading slightly exceed 2 per cent. The results of ray tracing and dynamic ray tracing in the new formulation should be considered superior, because linear interpolation of the elastic moduli $A_{\alpha\beta}^{(\xi)}$ conserves the TI character at any point of the model. For the standard ray tracing and dynamic ray tracing approaches, formulated in Cartesian coordinates, strict TI symmetry is only obtained along the isosurfaces on which the elastic moduli are specified. In between these surfaces the medium described by $A_{\alpha\beta}^{(x)}$ deviates slightly from TI.

10.4 Ray and dynamic ray tracing in model OR_{ROT}

Comparing the traveltimes, calculated using the procedure proposed in this paper, to those obtained by the standard ray tracing formulated in global Cartesian coordinates, we find a maximum deviation of approximately 2.5 per cent (Fig. 6, top panel). The traveltime deviations seem to be quite sensitive to the strength of the angular variation of the phase velocity. On the other hand, the traveltime deviations are quite insensitive to the inhomogeneity of the medium, that is, to the spatial variation of the elastic moduli. The relative differences for the spreading (Fig. 6, bottom panel) slightly exceed 4 per cent at depths ∼0.2 km, are close to zero at depths ∼0.7 km, and reach nearly 3 per cent at a depth

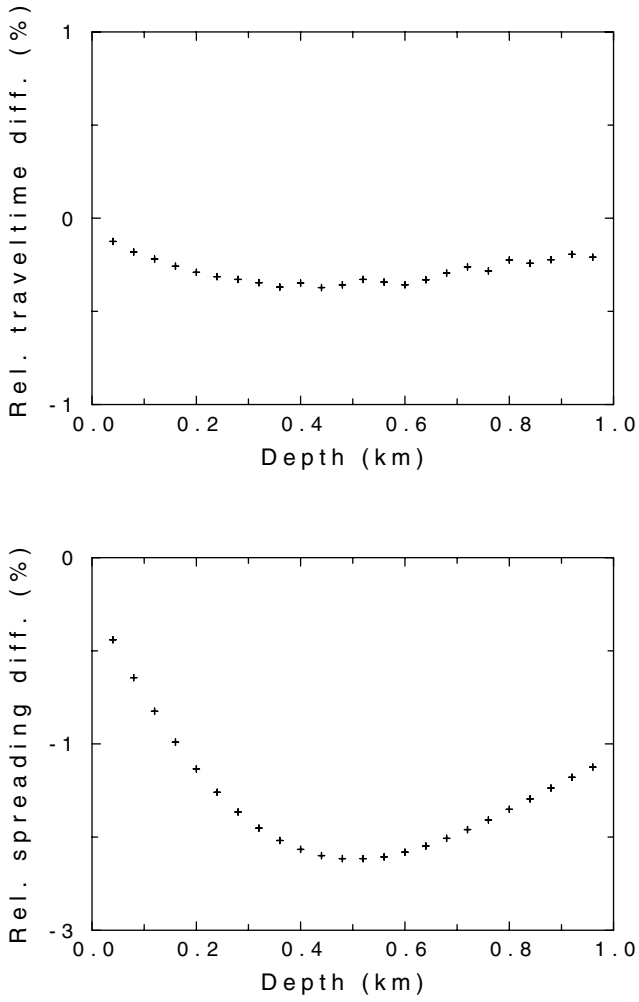

Figure 5. Relative differences in traveltime and geometrical spreading (in per cent) for the procedure proposed above and for the standard procedure, using model HTI_{ROT}.

of 1 km. Again, the results from the ray tracing with anisotropy formulated in curvilinear coordinates should be considered superior, because the linear interpolation of the elastic moduli $A_{\alpha\beta}^{(\xi)}$ and of the parametrizing functions of matrix **H** (angles λ, μ and ν) conserves the anisotropic symmetry at any point of the model.

11 CONCLUSIONS

We have introduced differential equations for ray tracing and inhomogeneous dynamic ray tracing, which allow efficient computations in anisotropic media with spatially varying symmetry elements (axes or planes). Although the proposed approach is generally applicable to media of arbitrary anisotropy, we foresee that its main use will be for anisotropic media of higher symmetry, for example, TI or OR symmetry. Our formulation, based on the knowledge of the minimum number of required elastic moduli $A_{\alpha\beta}^{(\xi)}$ in a curvilinear coordinate system, has a number of advantages compared to conventional ray tracing for anisotropic media, which is formulated with respect to the complete set of 21 elastic moduli $A_{\alpha\beta}^{(x)}$ in the Cartesian coordinate system.

The main reasons for introducing elastic moduli $A_{\alpha\beta}^{(\xi)}$ in a curvilinear coordinate system are enhanced efficiency of computations, smaller requirements of computer memory, possibilities for improved user-friendliness by utilizing simple relations between the elastic moduli $A_{\alpha\beta}^{(\xi)}$ and dimensionless anisotropy parameters (Thomsen 1986; Tsvankin 1997), and conservation of anisotropic symmetry during evaluation of functions $A_{\alpha\beta}^{(\xi)}(\mathbf{x})$. We emphasize that the proposed procedure is quite simple to implement if one already has available ray tracing and dynamic ray tracing procedures for a TI medium with a vertical axis or an OR medium where the symmetry planes are aligned with the main planes of the Cartesian coordinate system.

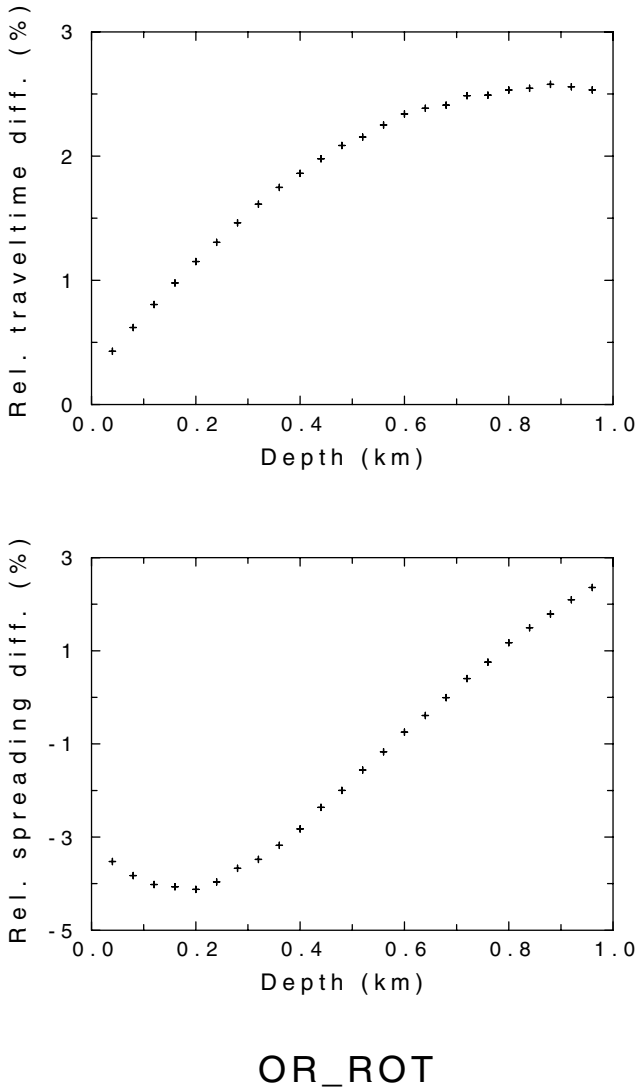

Figure 6. Relative differences in traveltime and geometrical spreading (in per cent) for the procedure proposed above and for the standard procedure, using model OR_{ROT}.

The efficiency of the proposed scheme can be illustrated on an example of a TI-symmetry medium with varying axis of symmetry. One integration step for the standard ray tracing procedure in Cartesian coordinates requires approximately 600 floating point operations (as for the lowest anisotropic symmetry), while the proposed scheme would require only around 350 operations. This is very rough estimate, which does not take into account the number of operations needed for evaluation of the volumetric functions and their derivatives.

In the numerical examples, we concentrated on ray tracing and homogeneous dynamic ray tracing procedures for P waves in smoothly varying media. The results seem to indicate that the relative differences between quantities computed with the use of the standard procedure (ANRAY) and the procedure proposed in this paper are greater for spreading, and thus for amplitudes, than for traveltime. Generalization of the proposed procedure for multiply reflected/transmitted and possibly converted elementary waves in layered media is expected to be quite straightforward. The procedure for the inhomogeneous dynamic ray tracing proposed above offers broad applications in various perturbation approaches. A combination of the proposed procedure with first-order ray tracing (Pšenčík & Farra 2005, 2007) and its generalization will offer further improvement of efficiency of ray tracing and dynamic ray tracing in heterogeneous, weakly anisotropic media. Application of the procedure to ray tracing and dynamic ray tracing along common *S*-wave rays (Bakker 2002) also seems straightforward.

ACKNOWLEDGMENTS

We are grateful to Peter Bakker, Tijmen Moser and an anonymous referee for valuable and stimulating comments. EI acknowledges the support of the Research Council of Norway, Project 174549/S30. IP acknowledges the support of the Consortium Project 'Seismic Waves in Complex 3-D Structures' and of Research Projects 205/05/2182 and 205/08/0332 of the Grant Agency of the Czech Republic.

REFERENCES

Bakker, P., 2002. Coupled anisotropic shear-wave ray tracing in situations where associated slowness sheets are almost tangent, *Pageoph,* **159,** 1403–1417.

Červený, V., 2001. *Seismic Ray Theory*, Cambridge Univ. Press, Cambridge.

Dehghan, K., Farra, V. & Nicolétis, L., 2007. Approximate ray tracing for qP-waves in inhomogeneous layered media with weak structural anisotropy, *Geophysics,* **72,** SM47–SM60.

Gajewski, D. & Pšenčík, I., 1987. Computation of high-frequency seismic wavefields in 3-D laterally inhomogeneous anisotropic media, *Geophys. J. R. astr. Soc.,* **91,** 383–411.

Iversen, E. & Pšenčík, I., 2007. Ray tracing for continuously rotated local coordinates belonging to a specified anisotropy, *Stud. Geophys. Geod.,* **51,** 37–58.

Isaac, J.H. & Lawton, D.C., 1999. Image mispositioning due to dipping TI media: a physical seismic modeling study, *Geophysics,* **64,** 1230–1238.

Lanlan, Y., Lines, L.R. & Lawton, D.C., 2004. Influence of seismic anisotropy on prestack depth migration, *First Break,* **23,** 30–36.

Pšenčík, I. & Farra, V., 2005. First-order ray tracing for qP waves in inhomogeneous weakly anisotropic media, *Geophysics,* **70,** D65–D75.

Pšenčík, I. & Farra, V., 2007. First-order P-wave ray synthetic seismograms in inhomogeneous weakly anisotropic media, *Geophys. J. Int.,* **170,** 1243–1252.

Schoenberg, M. & Helbig, K., 1997. Orthorhombic media: modeling elastic wave behavior in a vertically fractured earth, *Geophysics,* **62,** 1954–1974.

Thomsen, L., 1986. Weak elastic anisotropy, *Geophysics,* **51,** 1954–1966.

Tsvankin, I., 1997. Anisotropic parameters and P-wave velocity for orthorhombic media, *Geophysics,* **62,** 1292–1309.

Vestrum, R.W., Lawton, D.C. & Schmid, R., 1999. Imaging structures below dipping TI media, *Geophysics,* **64,** 1239–1246.